1. Classification *INPE-COM.10/PE*
C.D.U. 550.382.7

2. Period

4. Distribution Criterion
internal ☐
external X

3. Key Words (selected by the author)
ION PRODUCTION RATES,
ECLIPSE,
MAGNETIC ANOMALY.

5. Report Nº
INPE-1369-PE/173

6. Date
October, 1978

7. Revised by
J. A. Bittencourt

8. Title and Sub-title
ION PRODUCTION RATES DUE TO PARTICLE PRECIPITATION IN THE LOWER IONOSPHERE, OVER THE SOUTH ATLANTIC ANOMALY, FROM ROCKET ION COMPOSITION RESULTS DURING A TOTAL SOLAR ECLIPSE

9. Authorized by
Nelson de Jesus Parada
Director

10. Sector *DCE/DGA* Code *30.371*

11. Nº of Copies *17*

12. Authorship *M.A. Abdu*
Inez S. Batista
José H.A. Sobral

14. Nº of Pages *28*

13. Signature of the responsible

15. Price

16. Summary/Notes

Rocket results of ion densities during the 12 November 1966 total solar eclipse are analysed using detailed ion chemistry models for the D and E regions. Steady state continuity equation for the ionic species are solved to derive the ion production rates that can best explain the full sun ion composition results. The ion production rates so derived are inserted in a set of time dependent solutions of the continuity equation to predict the ion density distribution during the totality of the eclipse. By comparing calculated and observed ion densities during the totality we have determined the residual ion production rates, from which the part that can not be accounted for by solar radiation is attributed to the precipitation of high energy particles in the South Atlantic geomagnetic Anomaly.

17. Remarks *This work was partially supported by the "Fundo Nacional de Desenvolvimento Cientifico e Tecnológico - FNDCT" under contract FINEP-CT/271. This work will be submitted for publication, in Journal of Geophysical Research - JGR.*

ION PRODUCTION RATES DUE TO PARTICLE PRECIPITATION IN THE LOWER IONOSPHERE, OVER THE SOUTH ATLANTIC ANOMALY, FROM ROCKET ION COMPOSITION RESULTS DURING A TOTAL SOLAR ECLIPSE

M. A. Abdu, Inez S. Batista and José H. A. Sobral

Conselho Nacional de Desenvolvimento Científico e Tecnológico - CNPq
Instituto de Pesquisas Espaciais - INPE
12.200 - São José dos Campos, SP, Brazil

ABSTRACT

Results available on ion composition and electron densities, from the rocket measurements carried out during the total solar eclipse of 12 November 1966 at Cassino, Brazil, are subjected to a detailed numerical analysis using the presently known ion chemistry models for the D and E regions. Solutions of the continuity equations applicable to the individual ionic species are carried out under equilibrium conditions, to determine the ion production rates that can best represent the rocket measurements of the ion composition and electron density carried out to represent the full sun conditions. The ion production rates so derived are then inserted in a set of time dependent solutions of the continuity equations, to predict the ion density height distribution during the eclipse corresponding to the available rocket measurements. A comparison between the calculated results and the observations during the totality is then made to determine the residual ion production rates in the lower ionosphere, from which the part that can not be accounted for by solar radiation is attributed to the precipitation of high energy particles in the South Atlantic geomagnetic anomaly. The results are discussed in the light of the previous estimates of the ion production rates based on the nighttime occurrence of blanketing type E_s in the anomaly region.

1. INTRODUCTION

Measurements in the lower ionosphere, during a solar eclipse can provide valuable information on the many physical and chemical processes that operate in this region. The ion composition and electron density results during an eclipse represent an almost instantaneous picture of the balance between a rapidly changing solar ionizing radiation, on the one hand, and the response of the lower ionosphere on the other, the latter being dominated by a rather complex ion chemistry, including processes like recombination, attachment, detachment and charge neutralization. Therefore, if we know the ionization source function precisely and its variation during the eclipse, we can use the rocket measurements to deduce the rate coefficients of some important ion chemistry reactions. Such studies have been attempeted in the past. On the other hand, with a reasonable knowledge of the ion chemistry, one could reverse the procedure and proble into the nature of the ion production source functions. The present work is a attempt, on the latter procedure, to obtain a quantitative estimate of the source of ion production durng the totality of an eclipse. Since published results are available of a series of rocket flights conducted from Cassino, Brazil, situated inside the South Atlantic (also known as Brazilian) geomagnetic anomaly, during the total solar eclipse of 12 November 1966 (Narcisi et al., 1972; Ulwick, 1972; Mechtly et al., 1969), we were motived to investigate possible existence of an ion production source due to high energy particle precipitation in the geomagnetic anomaly. The ion composition and electron density data, available for the full sun and eclipse totality conditions, were subjected to a detailed numerical analysis in order to derive ion production rate distribution in the lower ionosphere. Then, using the results for the totality of the eclipse, we have isolated the possible ion production rates from the precipitation of high energy particles. The production rate profiles so derived could be used to construct an energy spectrum of the precipitating particles, though this is not attempted in the present work.

Our present knowledge of the aeronomic and ionospheric effects of charged particle precipitation in the geomagnetic anomaly is rather limited. Recent studies (Abdu and Batista, 1977 and Batista and Abdu, 1977) using sporadic E results obtained from an ionosonde operating in the anomaly region, have indicated evidence of particle precipitation on some "quiet" nights, and its significant enhancements following magnetic storms of moderate intensity. The results of the present work suggest that the particle ionization was a significant source under the quiet geomagnetic conditions during which the eclipse measurements were carried out.

2. METHOD OF ANALYSIS

Rocket results of the ion composition and electron densities in the height region of 75 km to 110 km, corresponding to the full sun conditions and during the totality of the eclipse, are used in the analysis. The first stage of the analysis is to determine the ion production rates, q's, that can best explain the full sun ion density profile, on the basis of the detailed ion chemistry schemes for the positive and negative ion compositions as they are presently known in this height region. The various q's, namely, $q(NO^+)$, $q(O_2^+)$, $q(O^+)$, $q(N_2^+)$ and $q(N^+)$, are determined as follows.

The $q(NO^+)$ is calculated for a representative solar Lyman α flux, using a nitric oxide height distribution derived from the $[NO^+]$ / $[O_2]$ ratio measured by the rocket. The remaining ion production rates are divided into two parts. One part consists of the $q(N_2^+)$, $q(O_2^+)$, $q(N^+)$ and $q(O^+)$ produced by the x-ray spectrum in the wavelength range of 1-100 Å as provided by Swider (1969). The other part consisting of only $q(O_2^+)$, produced by the solar Lyman β and EUV radiations acting on O_2 and $O_2^!$ (Δg), is then determined so that, togehter with the other production rates that are already known, it could explain the total ion density measured by the rocket. Such inference of the ion production rates involves solutions of the continuity equations of the individual ionic species, with the time derivative of their concentration assumed to be

zero. The ionization by particles is not considered in these initial calculations.

In a second stage of the present overall analysis the ion production rates for the full sun derived above are made to vary with time by using an eclipse obscuration function introduced in the time dependent solution of each continuity equation corresponding to each of positive and negative ion species. The total ion densities for the totality of the eclipse so obtained are then compared with their measurements during the totality. When the former is significantly smaller than the latter the difference is attributed to an extra source of ion production which has not been considered in the earlier derivations under full sun conditions. An estimate is made of this additional ion production rate which does not vary during the eclipse. The inclusion of this additional source in the pre-eclipse equilibrium solutions yields a modified set of electron production rates that now represents a better approximation to the correct production rates due to the solar radiation and the particles. These modified electron production rates are subsequently used in the time dependent solutions of the continuity equations and the resulting total ion densities during the eclipse totality are again compared with the observed values. By repeating the procedure we can determine the ion production rate due to particle ionization that gives a best fit between the calculated and observed ion density profiles during the totality of the eclipse.

3. ION CHEMISTRY REACTION SCHEMES

For positive ion chemistry we have used a detailed scheme that considers most of the species known to be present in the D and E regions. Above approximately 90 km the important ions are O_2^+, NO^+, N_2^+, N^+ and O^+, and heir chemistry is reasonably well understood in contrast to the situation at lower heights where the dominant species are hydrates of ions and cluster ions, many details of whose reaction processes are still not sufficiently understood. The part of the reaction

scheme leading to the formation of the ion hydrates, starting from the initial ion O_2^+, as proposed by Fehsenfeld and Ferguson (1969) and Ferguson (1971) is reasonably well established, as it is found to explain positive ion composition in the disturbed high latitude D region where O_2^+ is the dominant initial ion produced by precipitating protons (Narcisi, 1972). We have based our scheme on the work of these authors and have included some additional reactions and their coefficients as suggested by Swider and Narcisi (1975) and Mitra (1974). However, in the low latitude D region the reaction scheme that leads to the formation of ion hydrates starts from NO^+ which is considered to be the dominant initial ion. Somewhat detailed studies of this part of the reaction sequences have recently been carried out by Thomas (1976) and Reid (1977). The most important stages in the proposed schemes are: (i) the three body reactions of NO^+ to form $NO^+.CO_2$ and $NO^+.N_2$, (ii) the thermal break up of the latter ions and (iii) the switching reaction involving CO_2 to form $NO^+.CO_2$ from the weakly bound $NO^+.N_2$, as the precursors for the $NO^+.H_2O$ formation, from which successive hydration proceeds. The importance of the direct hydration of NO^+ as the precursor reaction relative to the CO_2 and N_2 channels depends upon the water vapour concentration and temperature in the D region (Reid, 1977). The reaction schemes and the rate coefficients adopted in the present calculations are in most part taken from Thomas (1976), and Reid (1977), and we have included the rate coefficients recently determined in the laboratory by Smith et al. (1977).

The negative ion reaction scheme is based on the 8 ion scheme taken from Reid (1970) and Swider and Keneshea (1972), including also the photo detachements of the major negative ions.

4. DETERMINATION OF THE FULL SUN ION PRODUCTION RATES BY SOLVING THE STEADY STATE CONTINUITY EQUATIONS

The continuity equations for each of the positive and negative ionic species are written down using the ion chemistry model discussed above and expressions for the equilibrium concentrations of these species are derived. Evaluations of these expressions require

the following inputs: (1) A knowledge of the production rates, from various sources, of the primary positive ions, NO^+, O_2^+, N_2^+, O^+ and N^+ which, however, are the parameters that we want to determine from these calculations. As a practical procedure we assume approximate production rates for these species (except for the production rate of 1-100 Å X-ray that was adopted from Swider (1969)) in the initial calculations and, by comparing the resulting ion densities with the observed values, the production rates were adjusted till the calculated and observed results agreed with each other. The details of the procedure will be clear in the course of the discussion to follow. (2) Height distributions of the major and minor atmospheric constituents, N_2, O_2, O, O_3, $O_2(^1\Delta_g)$ H_2O, H, OH, HO_2 and the temperature T. These were taken from Shimazaki and Laird (1972) for summer noon conditions. CO_2 concentration was taken as 3×10^{-4} $([O_2] + [N_2])$. For our calculation procedure we need also the measured ion densities and the $[NO^+] / [O_2^+]$ ratio to be compared with their calculated values. The mass spectrometer results of ion densities by Narcisi et al (1972) and the electron densities by Ulwick (1972) from Langmuir probe, and by Mechtly et al (1969) from radio method, to represent the full sun conditions for the time of the eclipse, show very good agreement above about 82 km, since these results were intercalibrated. We have used an average of the three results above 82 Km. Below this height, where the rocket results diverge, we have used the ion density results of Narcisi et al. The resulting ΣN_i^+ profile is shown in figure 1 (broken curve 1) and it coincides nearly exactly for most of the heights with the full sun ion density profile (solid curve 1) of Narcisi et al (1972). The height profile of $[NO^+]/[O_2^+]$ ratio for the full sun conditions taken from Narcisi et al (1972) is presented in figure 7 (solid curve 1).

Using the approximate production rates and the atmospheric model, (mentioned as inputs 1 and 2 above), we solve the coupled continuity equations for the individual positive and negative ionic species by iterating between the solutions of the positive species on the one hand, and the negative species on the other, and testing the charge neutrality condition, $\Sigma N_i^+ = [e] + \Sigma N_i$ at each step. The results are then compared with the observations, to derive the production rates of the dominant

primary ion species, $q(O_2^+)$ and $q(NO^+)$. As mentioned before, the ion production rates due to the X-rays of 1-100 Å that contribute a small fraction to the total $q(O_2^+)$ and most of $q(N_2^+)$, $q(O^+)$ and $q(N^+)$, were adopted from Swider (1969), as he has calculated these rates for quiet sun conditions, using an X-rays flux that was nearly equal to the flux measured by the NRL satellite (solar geophysical data, January 1967), for the eclipse day.

4.1. DETERMINATION OF $q(NO^+)$

The height distribution of $q(NO^+)$ is calculated for a solar Lyman α flux of 3 x 10" photons cm^{-2} sec^{-1}, based on the measurement by Smith et al (1972), using an $[NO]$ height distribution also deduced from the present calculation as follows. Evaluation of the expression for $[NO^+]/[O_2^+]$ for a set of heights using representative values of the relevant parameters, shows that, for a given set of raction rates this ratio depends on the production rate of NO^+ (denoted here as $P(NO^+)$), more than on any other parameter. The processes by which the first hydrate of the NO^+ is formed are also important in determining this ratio at height below 90 km. (For brevity of discussion, the relevant expressions are not given here). The sources of $P(NO^+)$ are (a) the direct photo ionization rate of NO by the solar Lyman α, $q(NO^+)$, and (b) charge transfer rate from the reaction $O_2^+ + NO \rightarrow NO^+ + O_2$, both of which are clearly directly proportional to the nitric oxide concentration. Also, the relative importance of (a) or (b) varies with height. The contribution to $P(NO^+)$ from the part (b), however, depend also upon $[O_2^+]$ and, hence, on $q(O_2^+)$. As a first step we assume that $q(O_2^+)$ is known (the evaluation of $q(O_2^+)$ will be discussed shortly) and evaluate the $[NO^+]/[O_2^+]$ ratio corresponding to a given $q(NO^+)$ which is approximate to start with. We then adjust the $[NO]$ by making to agree the calculated and observed results of $[NO^+]/[O_2^+]$ ratio. The resulting $[NO]$ is subsequently used to calculate a more correct $q(NO^+)$ and the procedure is repeated. The $[NO]$ and $q(NO^+)$, determined in this way will be a true representation of the observed ion densities only if the assumed $q(O_2^+)$ is correct.

4.2. DETERMINATION OF $q(O_2^+)$

The $q(O_2^+)$ is evaluated by comparing the measured and calculated total ion densities. Since a tentatively correct $q(NO^+)$ was determined in the previous step and since the q's due to X-ray of 1-100 Å are already known, the only remaining ion production rate $q(O_2^+)$ can be estimated by adjusting it so that the calculated total ion density is equal to the observed value. The resulting $q(O_2^+)$ is then used in the previous step to obtain a revised $q(NO^+)$, which is a better approximation to its correct value. Thus, by iterating between the two steps, we can calculate $q(O_2^+)$, $q(NO^+)$ (and $[NO]$) that best explain the observed total ion density and the $[NO^+]/[O^+]$ ratio, respectively.

The height distribution of the full sun total and individual production rates of the initial ions deduced here, and those adopted for the 1-100 Å X-rays, are plotted in figure 2. The contribution from the latter to the total ion production varies from 10 to 20 percent, depending upon height, and hence its influence on the deduced $q(O_2^+)$ and $q(NO^+)$ is not very significant. The zenith angle of the sun during the ion density measurements was around 18^o. It is interesting to note that the transition height below and above which the dominant primary ions produced are NO^+ and O_2^+, respectively, is around 84 km in figure 2, which is about 10 km lower than in the ion production rate profiles for the solar minimum conditions and solar zenith angle 60^o, given by Sechrist (1972) and Thomas (1974), both of whom have based their $q(NO^+)$ values on the $[NO]$ height distribution of Meira (1971). The total ion density (ΣN_i^+), and $[O_2^+]$ and $[NO^+]$, that resulted from these ion production rates, are presented in figure 3 which,as per the calculation procedure, corresponds to the broken curve 1 in figure 1 and the solid curve 1 in figure 7, respectively. Some details of the ion composition that resulted from this calculation are also presented in the same figure. It is seen that water cluster ions are dominant below about 82 km, which is in agreement with the results of Narcisi et al (1972). Only a limited agreement between the calculation and measurements is present in the relative distribution of the various species, the most notable of which is in the height of the peak of $[H_3O^+]$ and in the height distribution of $[H_7O_3^+]$. Our results, showing $NO^+.H_2O$ as the most abundant water cluster ion above 76 km,

desagrees with the results of Narcisi et al (1972), which shows $H_5O_2^+$ as the most abundant species. However, significant concentration of the first hydrate of NO^+ in this height region has been obtained in the theoretical estimations by Thomas (1976) and Reid (1977), and have also been detected in some rocket measurements (Johannsen and Krankowsky,(1972) and Zbinden et al (1975). With the existing uncertainty in the rocket technique of composition measurement of the leavey cluster ions, and our limited knowledge of the several reaction coefficients used in the chemical scheme, the possibility seems to be very limited of a better agreement between the observational and theoretical results. However, this disagreement in the relative concentration of the cluster ions will have only negligible influence on our results, which will be based on ΣN_i^+ .

5. TIME DEPENDENT SOLUTION OF THE CONTINUITY EQUATIONS TO DETERMINE ION DENSITY PROFILES DURING THE ECLIPSE

The ion production rates, determined in section 4, are varied through the eclipse, using an eclipse obscuration function, defined as the ratio R(t) of the uneclipsed area to the total area of the solar disc, given by

$R(t) = \frac{1}{\pi} (\pi - \theta(t) + \sin \theta\ (t))$, where $\cos \theta\ (t) = 1 + 8\ t\ (t/T - 1)/T$.

Here t is the time from the first contact, T is the eclipse duration and θ is the angle at the center of the solar disc circle subtended by the points of intersections between the lunar and the solar disc circles. The ion production rate function, so determined, is used in a time dependent solution of the system of continuity equations. The residual ion production rates of the various species during the totality of the eclipse were taken into account by assuming that they were proportional to the responsible ionizing radiations, the residual fluxes of which were taken as 5.2 percent for X-rays 1-10Å, 16 percent for X-rays 30-100Å (Accardo et al. 1972) and 0.52 percent for Lyman α and Lyman β (Smith et al. 1972). Numerical solutions of the continuity equations for all the ion species were carried out using the relationship, $N^{\pm}_{ji} = N^{\pm}_{ji-1} + (P_{ji-1} - L_{ji-1})\ \Delta t$, where $N^{\pm}_{ji}$ is the concentration of the jth ion species, positive or negative, at the ith time step of integration and P_{ji} and L_{ji} are the corresponding production and loss rates, respectively. The interval between the time steps, Δt, is

taken as 1 second in our calculation. The solution of the equation for each of the ion species was carried out in succession somewhat in the way in which the reactions proceed in the chemical scheme and, at the end of each time step, the charge neutrality condition, $\sum_j N^+_{ji} = \sum_j N^-_{ji} + [e]_i$ was tested. In the case of ion species having lifetimes less than a second, the equilibrium solutions were maintained. The atmospheric model used in the calculation was assumed unchanging during the eclipse, except for [O] and $[O_3]$ below 90 km, which we adopted from Thomas and Bowman (1974) after normalizing to the preeclipse values.

The total positive ion density profiles obtained from the calculation, for 80 percent obscuration of the sun and for the total obscuration, are plotted as broken curves 2 and 3 respectively in figure 1, where solid curves (2) and (3) are the corresponding observed profiles from Narcisi et al. (1972). In the case of the solid curve (3), we have used the totality electron density results of Mechtly et al. (1969), for heights above 95 km, since Narcisi et al. did not measure ion densities at these heights and their results for full sun conditions agree well with those of Mechtly et al. between 82 and 95 km. It can be observed in figure 1 that the calculated ion densities are smaller than the observed values, in the cases of 80 percent and total eclipse, except between 85 and 90 km where the calculated results attain higher values. Two possible explanations for the latter results can be considered as follows: (a) The production rates due to the short X-rays that ionize this height region might have undergone variations during the course of the eclipse, not included in our calculations. Such a possibility is very remote since the sun was quiet and no minor X-ray event was reported by the NRL solar monitoring satellite for this day (Solar Geophysycal Data, January 1967). (b) The rate coefficients used for certain reactions that eventually control the loss rate of the ionization, might be thought to contribute to the difference. But the difference found below 85 km, namely, calculated values being lower than the observed values, does not conform to this possibility. If however certain key reaction rates are temperature sensitive, then a possible change in the shape of the mesospheric temperature profile, during the eclipse, could conceivably produce this type of behaviour in the ion density profiles. The three body reaction rates for formation of the

first hydrate of NO^+, directly from NO^+ and through processes involving N_2 and CO_2, are known to be highly temperature dependent (Smith et al 1977, Reid 1977). As is the case of the three body reaction to form O_4^+ from O_2^+ (Payzant et al 1973). The consequence of a decrease in the temperature will be to enhance the rate of formation of the cluster ions, that are known to recombine faster than the simple molecular ions. However, no observational data exists at present to judge the validity of the hypothesis of a mesospheric temperature change during an eclipse. The above discussion demonstrates the complex nature of the ion chemistry below 90 km and a full discussion of this part of the results would have to await availability of further relevant information in this height region.

Above 90 km the ion chemistry is much better understood, and the significant reduction in the calculated ion density, relative to the measurements for the 80 percent and the total eclipse can be explained in terms of ion production rates, as shown in the next section.

6. DERIVATION OF THE ION PRODUCTION RATE DUE TO PARTICLE IONIZATION

The difference between the calculated and observed ion densities above 90 km for both the 80 percent and the total eclipse, in figure 1, appears significant. We have attributed this difference to the fact that we did not include, in our calculations, an important additional source of ionization. This source of ionization which we attribute to particle ionization, q_p, is evaluated as follows. Given solar ionization contribution during the totality of the eclipse, as shown in the previous section, we can estimate an approximate q_p necessary to obtain an approximate fit between the calculated and observed ion density during the eclipse totality. This approximate q_p is introduced into the calculations under equilibrium and full sun conditions, to yield a modified set of ion production rates due to solar radiation, so that consequently the full sun ion densities, and the $[NO^+]/[O_2^+]$ ratio can, as well, be explained by these modified solar ion production rates and q_p. The new set of ion production rates is then inserted in the time dependent solution of the continuity equation, with q_p as a time independent component. The result of the total ion density during the

eclipse totality obtained from this calculation is then compared with the observed values and, depending upon the difference between the two results, q_p is modified, and the above procedure repeated until we obtain agreement between the calculated an the observed results. The final results are presented in figure 4, where the calculated (broken curve 3) and observed (solid curve 3) ion densities are shown for the eclipse totality. For the 80 percent eclipse, the calculated values are still smaller than observed, above 95 km. The resulting ion production rates are presented in figure 5. q_T represents the sum of q_p and the ion production rates due to solar radiation for the full sun conditions. q_r is the residual solar ion production rate that was present during the totality of the eclipse. The contribution made by q_p is seen to be nearly an order of magnitude higher than the residual ion production rate above 96 km. For a comparison we have plotted, in the same figure, the ion production rates due to the scattered Lyman α and Lyman β radiations calculated by Ogawa and Tohmatsu (1966), which is found to be a factor of 50 to 100 less than q_r.

7. DISCUSSION OF THE RESULTS

The method of deriving the q_p, the production due to particle ionization, described here, is based upon the determination of the ion production rates due to solar radiation that are required to explain the ion densities measured for full sun conditions. Therefore, the only likely errors in our determination of q_p would be those that depend upon the accuracy of the ionization density measurements and upon possible changes, during the eclipse, of the parameters in the atmospheric model used for the calculations. Mechtly et al. (1969) estimate an error of 15% in their electron density measurements, by the Faraday rotation technique, above 90 km. The resulting error bar is indicated on the q_p curve in figure 5. The atmospheric parameters whose variations during the eclipse might affect our q_p determination are $[NO]$ and the temperature; $[NO]$, through its role in the formation of $[NO^+]$ by the charge transfer reaction with $[O_2^+]$; and the temperature, due to the temperature dependent recombination coefficients of O_2^+ and NO^+. Nothing appears to be known about the eclipse variations in $[NO]$. We assume it to be not significant.

Since the dissociative recombination coefficients of O_2^+ and NO^+ are inversely proportional to the temperature, (Biondi (1973)) any possible decrease in T during the eclipse will have the effect of increasing the recombination rates and the inclusion of this effect, if it exists, would be to revise upward the calculated q_p.

The following considerations on the measured and calculated ratio $[NO^+]/[O_2^+]$ also suggest the presence of a significant extra source of particle ionization in the eclipse measurements. Figure 6 shows the results of our time dependent calculation of $[NO^+]/[O_2^+]$ for 76 km, 80 km, 100 km and 110 km. For the latter two heights the ratio, calculated on the basis of the solar radiation only, shows large enhancements (solid line), as expected, during the eclipse totality. The inclusion of q_p in the calculation is such that the $[NO^+]/[O_2^+]$, near the totality of eclipse, is significantly lowered (broken curve) and appears to have approached the expected values at these heights, as per the measurement by Narcisi et al. (1972). A height profile of the same feature is illustrated in figure 7, showing these ratios for the full sun, 80 percent eclipse and the totality of the eclipse. In the case of eclipse totality we have shown the $[NO^+]/[O_2^+]$ profile for the two cases, namely, q_p included and $q_p = 0$. When q_p is included in the calculation, the ratio $[NO^+]/[O_2^+]$ is reduced and it approches the values measured by Narcisi et al. (1972).

In a recent study by Abdu and Batista (1977), an attempt was made to estimate ion production rates due to particle precipitation, that might be regularly present, to explain the occurrence of nighttime sporadic E layers of the blanketing type. The result showed that the monthly average particle ion production rate, for the period studied, was about two orders of magnitude larger than the ion production rates due to the scattered Lyman β radiation, calculated by Ogawa and Tohmatsu (1966). The present result shows that, on the day of the eclipse, a relatively quiet day, the ion production rate q_p was about 200-500 times that due to the scattered UV radiation in the lower E region. However, the q_p deduced here is significantly less than we have deduced from observations of enhancements in the blanketing frequency of the E_s

layer during disturbed periods following magnetic storms (Batista and Abdu 1977).

8. CONCLUSIONS

We have analysed the results on the ion composition and electron densities, available from the rocket observational campaign conducted over Cassino, South Brazil, during the total solar eclipse of 12 November 1966, in order to infer quantitatively a possible ion production rate due to precipitation of charged particles in the upper atmosphere over the South Atlantic geomagnetic anomaly. The results for the totality of the eclipse have been used in our derivations since under this condition the component of ion production due to sources other than solar radiation becomes pronounced, making its detection easier. The method of analysis used is as complete as possible, within the present understanding of the ion chemistry of the lower ionosphere. The normalization of the ion production rates due to the solar radiation, to the rocket observed full sun ion density profiles, makes the results of our analysis somewhat free from possible deficiencies of an assumed atmospheric model. The results of our analysis show that below about 90 km the interpretation and the utilization of the rocket results for the derivation of the ion production rate become difficult, because of the complex nature of the positive ion chemistry in this part of the lower ionosphere. Since the reaction rates in the hydration process of the NO^+ is highly temperature dependent, as is believed at present, our analysis results might seem to indicate the possibility of mesospheric temperature change during the eclipse. Further studies of these aspects are continuing.

Above 90 km, where the chemical processes are reasonably well understood, a comparison between the results of our calculations and rocket data during the total eclipse clearly indicate the presence of ion production due to source other than direct and scattered solar radiation. This source , which we attribute to particle precipitation, has been found to be significant during the quiet conditions under which the eclipse measurements were carried out. The deduced ion production rate in the lower E region is a factor of 2-5 higher than a previous

estimate, also during quiet conditions, carried out using the sporadic E results in the region of the geomagnetic anomaly. It should be borne in mind, however, that the present determination of q_p corresponds to a period near the solar activity maximum (Nov. 1966), while our earlier estimates from the E_s results were made near the minimum of the solar activity cycle (1973-74), which could result in different production rates by particle ionization.

ACKNOWLEDGEMENTS

This work was partially supported by Fundo Nacional de Desenvolvimento Científico e Tecnológico (FNDCT) by contract FINEP-271 CT. The authors are grateful to Drs. A. P. Mitra and C. F. Sechrist who made useful comments on the original manuscript that was presented at the STP symposium in June 1978 in Austria. We are also thankful for useful discussions with Dr. Volker W. J. H. Kirchhoff.

REFERENCES

ABDU, M.A. and I.S. BATISTA., Sporadic E-layer phenomena in the Brazilian geomagnetic anomaly: evidence for a regular particle ionization source. *J. Atmos. Terr. Phys.*, 39, 723-731, 1977.

ACCARDO, C.A. L.G. SMITH and G.A. PINTAL., Rocket observations of solar X-rays during the eclipse of 7 March 1970. *J. Atmos. Terr. Phys.*, 34, 613-620, 1972.

BATISTA, I.S. and M.A. ABDU., Magnetic storm associated delayed sporadic-E enhancements in the Brazilian geomagnetic anomaly. *J. Geophys. Res.*, 82, 4777-4783, 1977.

BIONDI, M.A., The effects of ion complexity on electron-ion recombination. *Comments At. Mol. Phys.*, 4, 85-91, 1973.

FEHSENFELD, F.C. and E.E. FERGUSON., Origin of water cluster ions in the D-region. *J. Geophys. Res.*, 2217-2222, 1969.

FERGUSON, E.E., Laboratory measurements of D-region ion-molecule reactions, in: *Mesospheric Models and Related Experiments*, ed. G. Fiocco, pp. 188-197, D. Reidel, Dordrecht, Netherlands, 1971.

JOHANNESSEN, A. and D. KRANKOWSKY., Positive ion composition measurements in the upper mesosphere and lower thermosphere at a high latitude during summer. *J. Geophys. Res.*, 77, 2888-2901, 1972.

MECHTLY, E.A., K. SEINO, and L.G. SMITH., Lower ionosphere electron densities measured during the solar eclipse of november 12, 1966. *Radio Science*, 4, 371-375, 1969.

MEIRA, L.G., Jr., Rocket Measurements of upper atmospheric nitric oxide and their consequences to the lower ionosphere. *J. Geophys. Res.*, 76, 202-212, 1971.

MITRA, A.P., *Ionospheric effects of solar flares.* D. Reidel Publishing Company, Dordrecht-Holland, 1974.

NARCISI, R.S., Aeronomic implications from ion Composition Measurement during a PCA. *Proceedings of COSPAR Symposium on Solar Particle Event of November 1969.* AFCRL-72-0474. Air Force Cambridge Res. Lab. Bedford Mass., 1972.

NARCISI, R.S., A.D. BAILEY, L.E. WLODYKA and C.R. PHILBRICK., Ion Composition measurements in the lower ionosphere during the November 647-658, 1972.

OGAWA, T. and T. TOHMATSU., Photoelectronic processes in the upper atmosphere , II. The hydrogen and helium ultraviolet glow as on origin of the nightime ionosphere. *Rep. Ionos. Space. Res. Jap.*, 20 395-417, 1966.

PAYZANT, J.D., A.J. CUNNINGHAN and P. KEBARLE., Temperature dependence of the rate constants for the third order reaction: $O_2^+ + 2O_2 \rightarrow O_4^+ + O_2$ and $O_4^+ + 2O_2 \rightarrow O_6^+ + O_2$. *J. Chem. Phys.*, 59, 5615-5619, 1973.

REID, G.C., Production and loss of electrons in the quiet daytime D-region of the ionosphere. *J. Geophys. Res.*, 75, 2551-2562, 1970.

REID, G.C., The production of water cluster positive ions in the quiet daytime D-region. *Plan. Space Sci.*, 25, 275-290, 1977.

SECHRIST, JR., C.F., Theoretical models of the D-region. *J. Atmos. Terr. Phys.*, 34, 1565-1589, 1972.

SHIMAZAKI, T. and A.R. LAIRD., Seasonal effects on distributions of minor neutral constituents in the mesosphere and lower thermosphere. *Radio Sci.*, 7, 23-43, 1972.

SMITH, D., N.G. ADAMS and D. GRIEF., Implications of some laboratory determinations of NO^+ reaction rates to cluster ion formation in the D-region. *J. Atmos. Terr. Phys.*, 39, 531-521, 1977.

SMITH, L.G., Rocket observations of solar UV radiation during the eclipse of 7 March 1970. *J. Atmos. Terr. Phys.*, 34, 601-611, 1972.

SWIDER, W., Ionization rates due to the attenuation of 1-100 Å nonflare solar X-rays in the terrestrial atmosphere. *Rev. Geophys.*, 7, 573--594, 1969.

SWIDER, W. and R.S. NARCISI., A study of the nighttime D-region during a PCA event. *J. Geophys. Res.*, 80, 655-664, 1975.

SWIDER, W. and T.J KENESHEA., Diurnal variation in the D-region during PCA events. *Proc. COSPAR Symp. on Solar Particle event of November 1964, ed. J.C. Ulwick, AFCRL-72-0474*, 589-636, 1972.

THOMAS, L., Recent developments and outstanding problems in the theory of the D-region. *Radio Sci.*, 9, 121-136, 1974.

THOMAS, L. NO^+ and water cluster ions in the D-region. *J. Atmos. Terr. Phys.*, 38, 61-67, 1976.

THOMAS, L. and M.R. BOWMAN., Changes in concentrations of oxygen and hydrogen constituents in the mesosphere during an eclipse. *J. Atmos. Terr. Phys.*, 36, 1421-1426, 1974.

ULWICK, J.C., Eclipse rocket measurements of charged particle concentrations. *J. Atmos. Terr. Phys.*, 34, 659-665, 1972.

ZBINDEN, P.A., M.A. HIDALGO, P. EBERHARDT and J. GEISS., Mass spectrometer measurements of the positive ion composition in the D and R-region of the ionosphere. *Plan. Spac. Sci.*, 23, 1975.

FIGURE CAPTIONS

Figure 1 - Height profiles of the ion densities measured by Narcisi et al. (1972) and those calculated in this paper. The solid lines (1), (2) and (3) are the measurements for the full sun, 80 percent eclipse, and the totality, respectively. The part of curve 3 above 96 km is taken from Mechtly et al. (1969). The profiles represented by broken curves 2 and 3 are the results of the time dependent solutions for 80 percent eclipse and for the totality, respectively. The broken curve (1) represents the ion density used in deriving the ion production rates shown in Figure 2.

Figure 2 - The ion production rates $q(NO^+)$, $q(O_2^+)$ that were derived, and $q(N_2^+)$, $q(O^+)$ and $q(N^+)$ from short X-rays taken from Swider (1969), to explain the full sun ion density profile represented by curve 1 in Figure 1, when the ion production rate due to particle ionization is not considered.

Figure 3 - Height profiles of the positive ion composition obtained from the calcutations.

Figure 4 - The ion density profiles, for the cases shown in Figure 1 after fitting the calculated results with the observation at the totality of the eclipse, as explained in the text. The identifications of the curves are the same as in Figure 1.

Figure 5 - Ion production rates calculated after including the component due to particle precipitation to explain the eclipse totality results. The height profile of this component is marked as q_p. q_R is the ion production rate due to the residual solar radiation during the totality of the eclipse. q_T is the total ion production rate, that includes the q_p and the ion production rate due to solar radiation q_s, that explain the ion density profile for the uneclipsed sun. The curves marked L_β and L_α are the ion production rates due to the scattered UV radiation

calculated by Ogawa and Tohmatsu (1966).

Figure 6 - Variation of the ratio $[NO^+]/[O_2^+]$ during the eclipse, calculated excluding the q_p (solid line) and including the q_p (broken line).

Figure 7 - Height profiles of the ratio $[NO^+]/[O_2^+]$. Curves 1, 2 and 3 represent the measurements by Narcisi et al for the full sun, 80 percent eclipse and the totality respectively. Curves 3a and 3b represent the calculated results for the totality, excluding the q_p and including the q_p respectively.

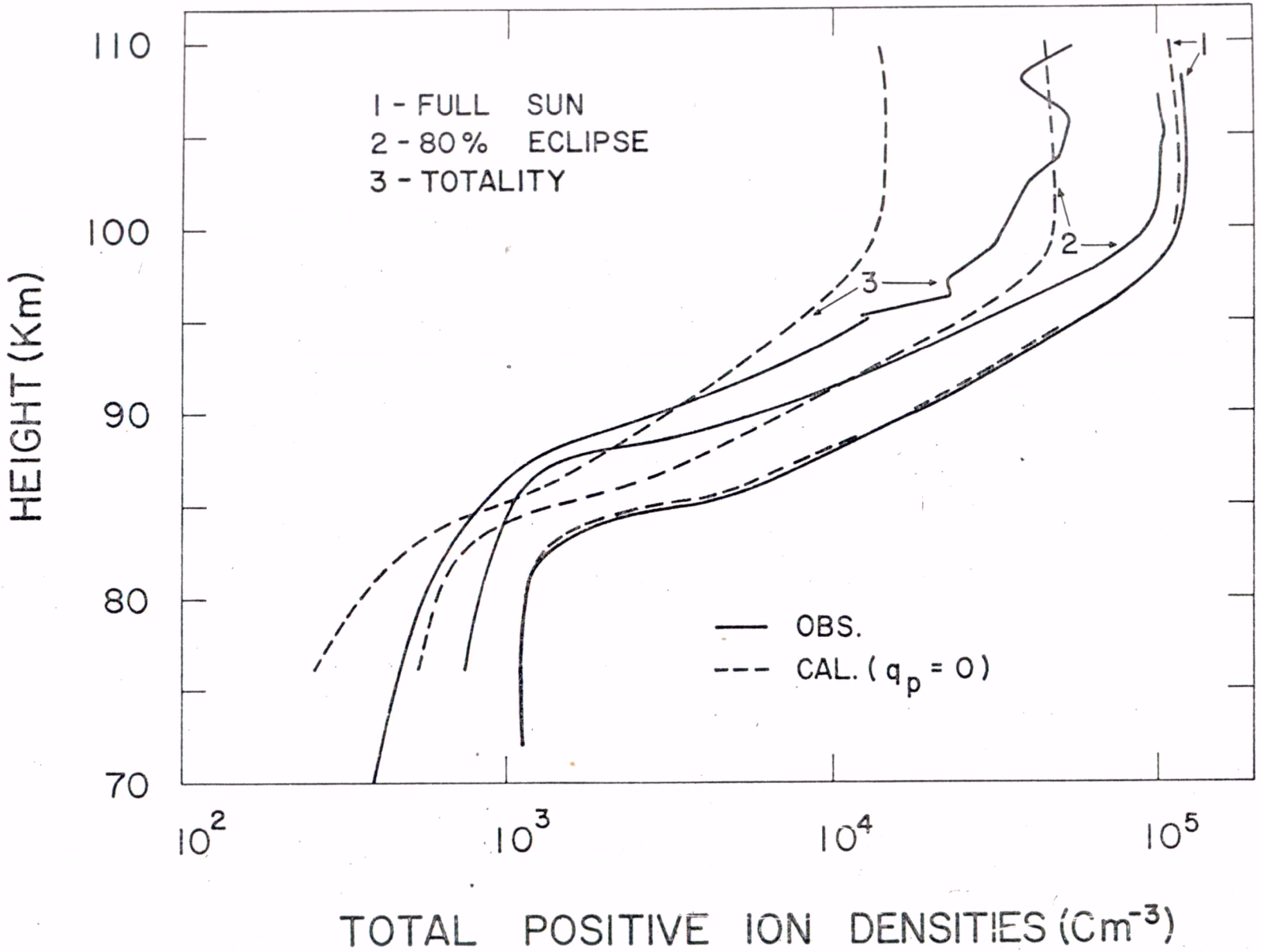
1 - FULL SUN
2 - 80% ECLIPSE
3 - TOTALITY
OBS.
CAL. ($q_p = 0$)
HEIGHT (Km)
110
100
90
80
70
10^2
10^3
10^4
10^5
TOTAL POSITIVE ION DENSITIES (Cm^{-3})

FIG. 1

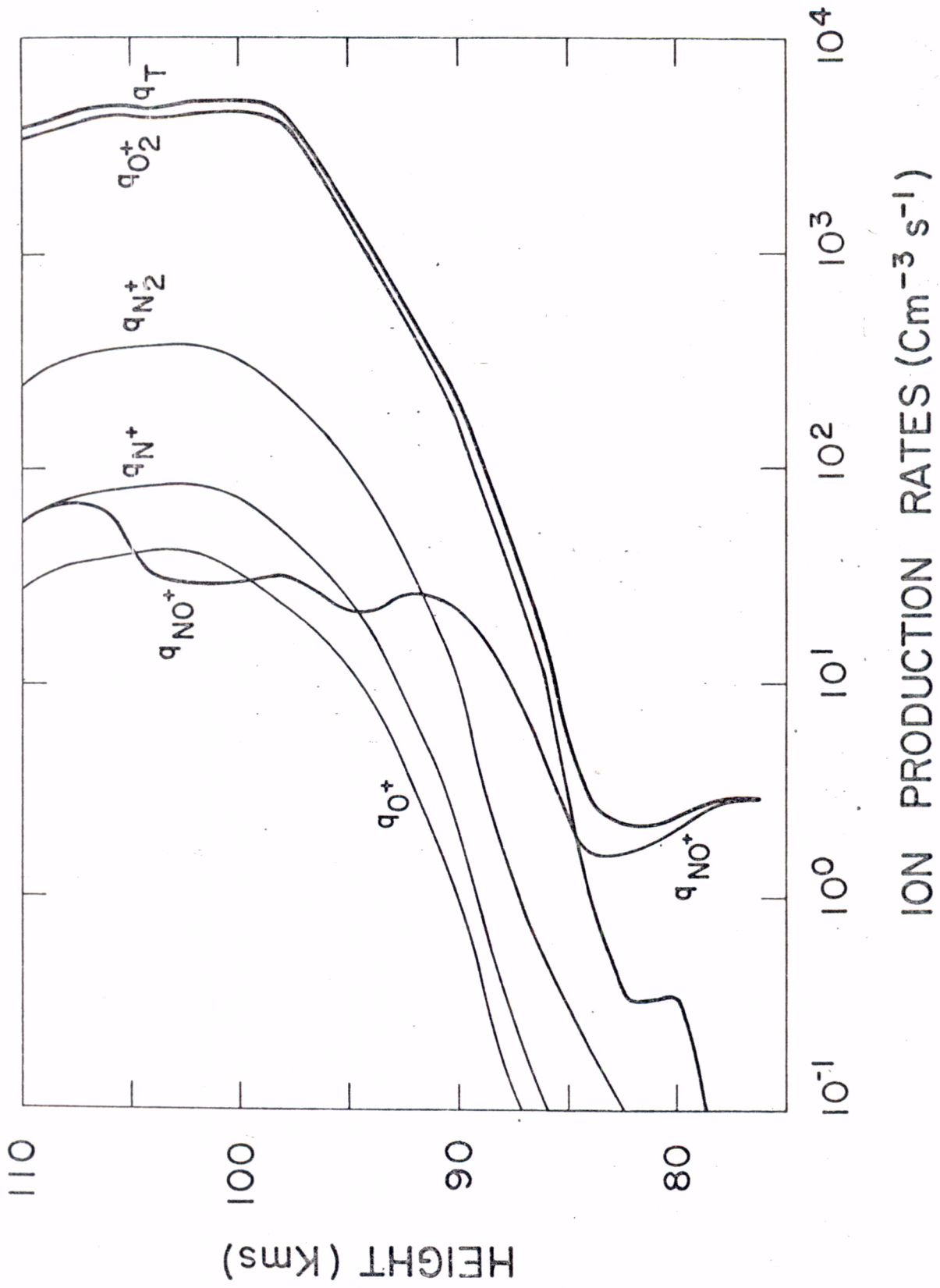

FIG.2 - The ion production rates $q(NO^+)$, $q(O_2^+)$ that were derived, and $q(N_2^+)$, $q(O^+)$ and $q(N^+)$ from short X-rays taken from Swider (1969), to explain the full sun ion density profile represented by curve 1 in Figure 1, when the ion production rate due to particle ionization ins not considered.

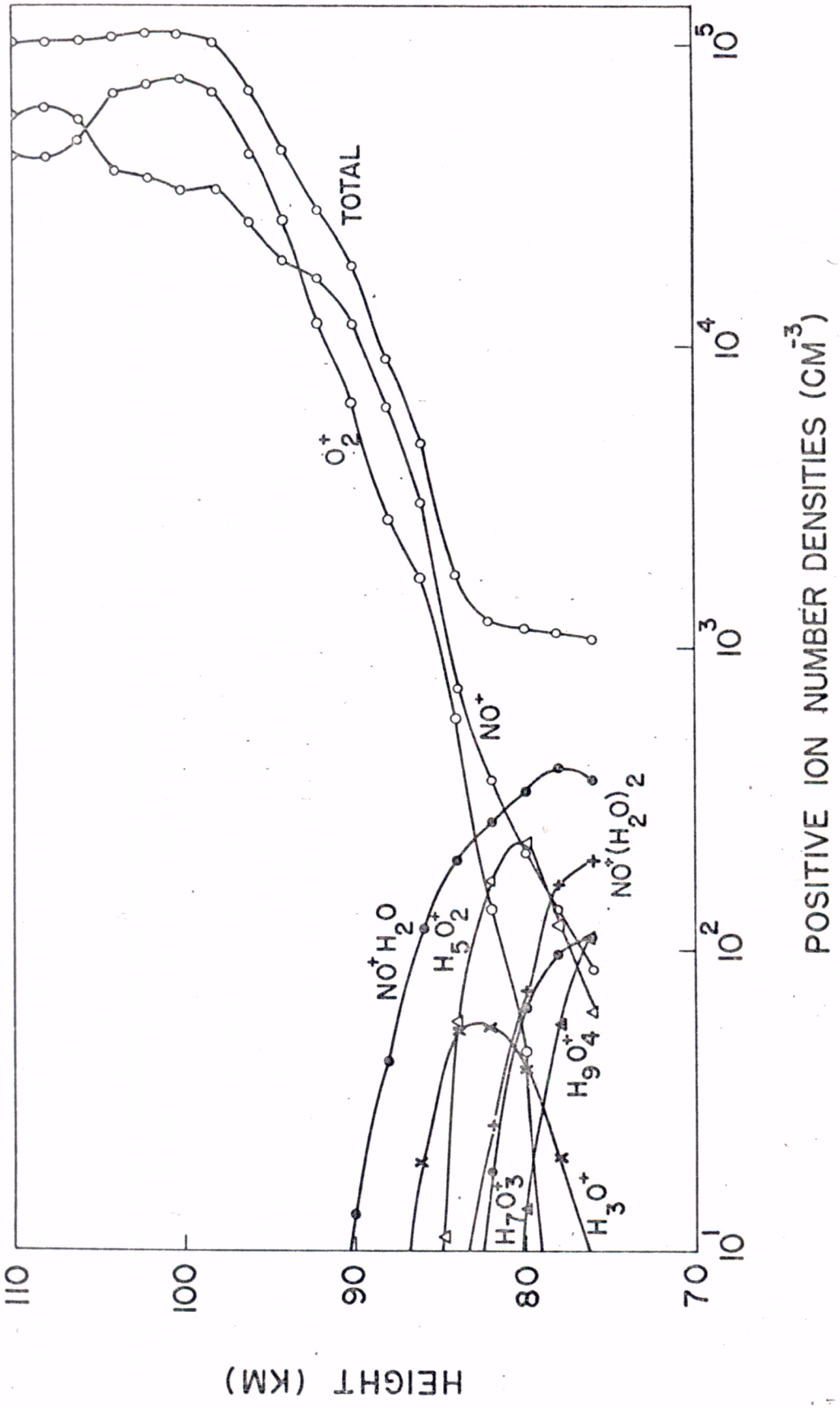

FIG. 3 - Height profiles of the positive ion composition obtained from the calculations.

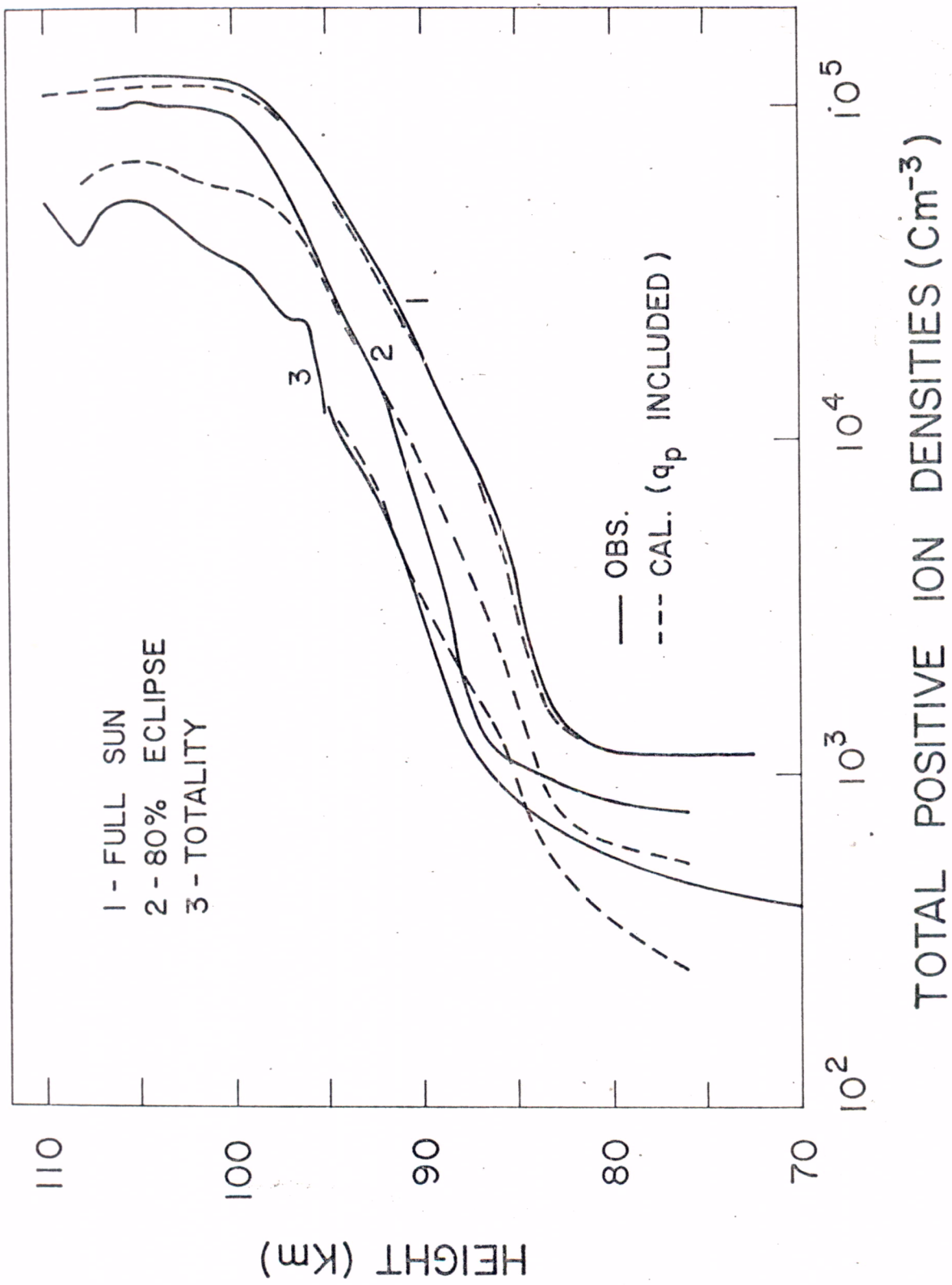

FIG. 4 - The ion density profiles, for the cases shown in Figure 1 after fitting the calculated results with the observation at the totality of the eclipse, as explained in the text. The identifications of the curves are the same as in Figure 1.

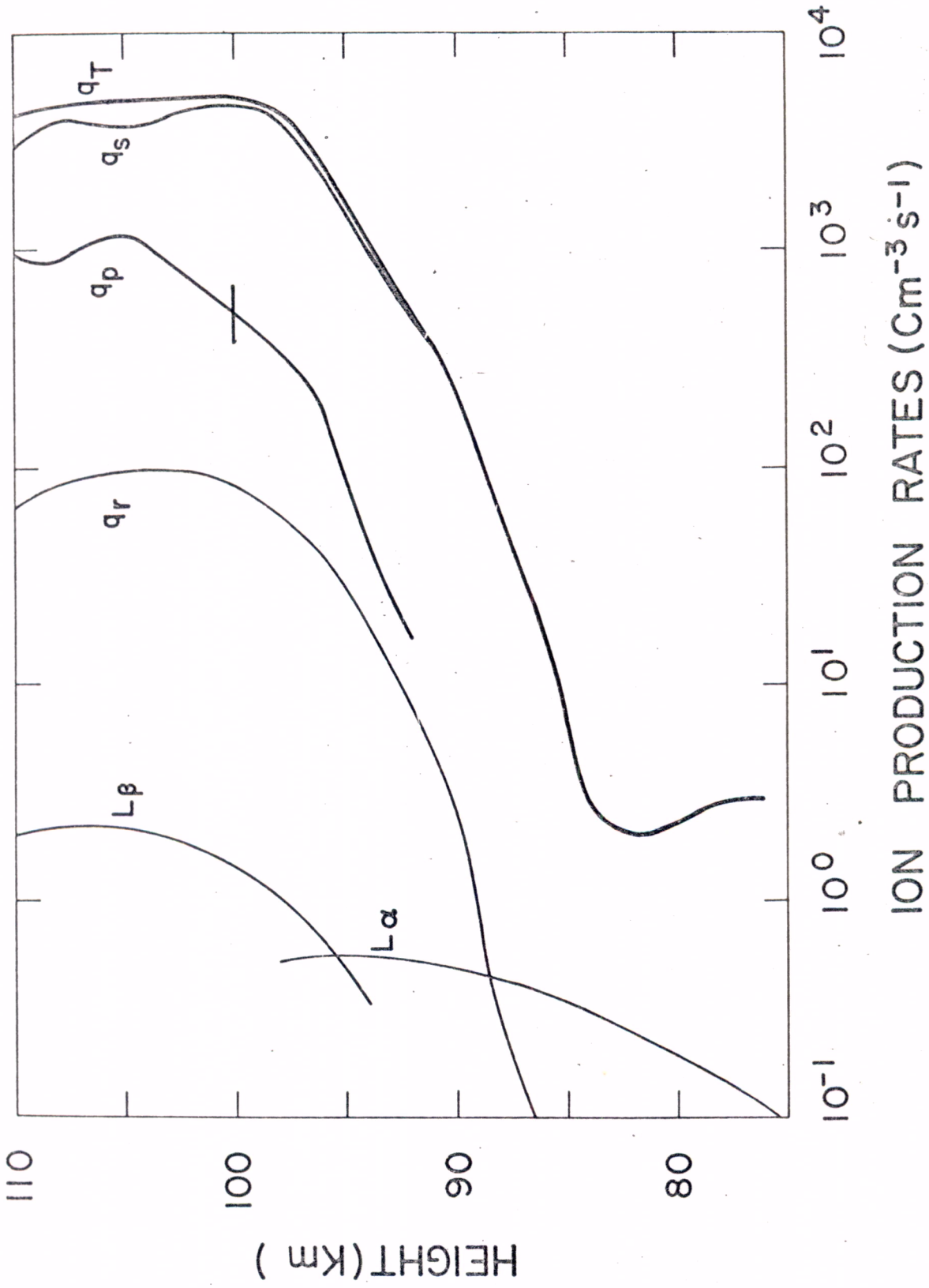

FIG. 5 - Ion production rates calculated after including the component due to particle precipitation to explain the eclipse totality results. The height profile of this component is marked as q_p. q_R is the ion production rate due to the residual solar radiation during the totality of the eclipse q_T is the total ion production rate, that includes the q_p and the ion production rate due to solar radiation q_s that explain the ion density profile for the uneclipsed sun. The curves marked L β and L α are the ion production rates due to the scattered UV radiation calculated by Ogawa and Tohmatsu (1966).

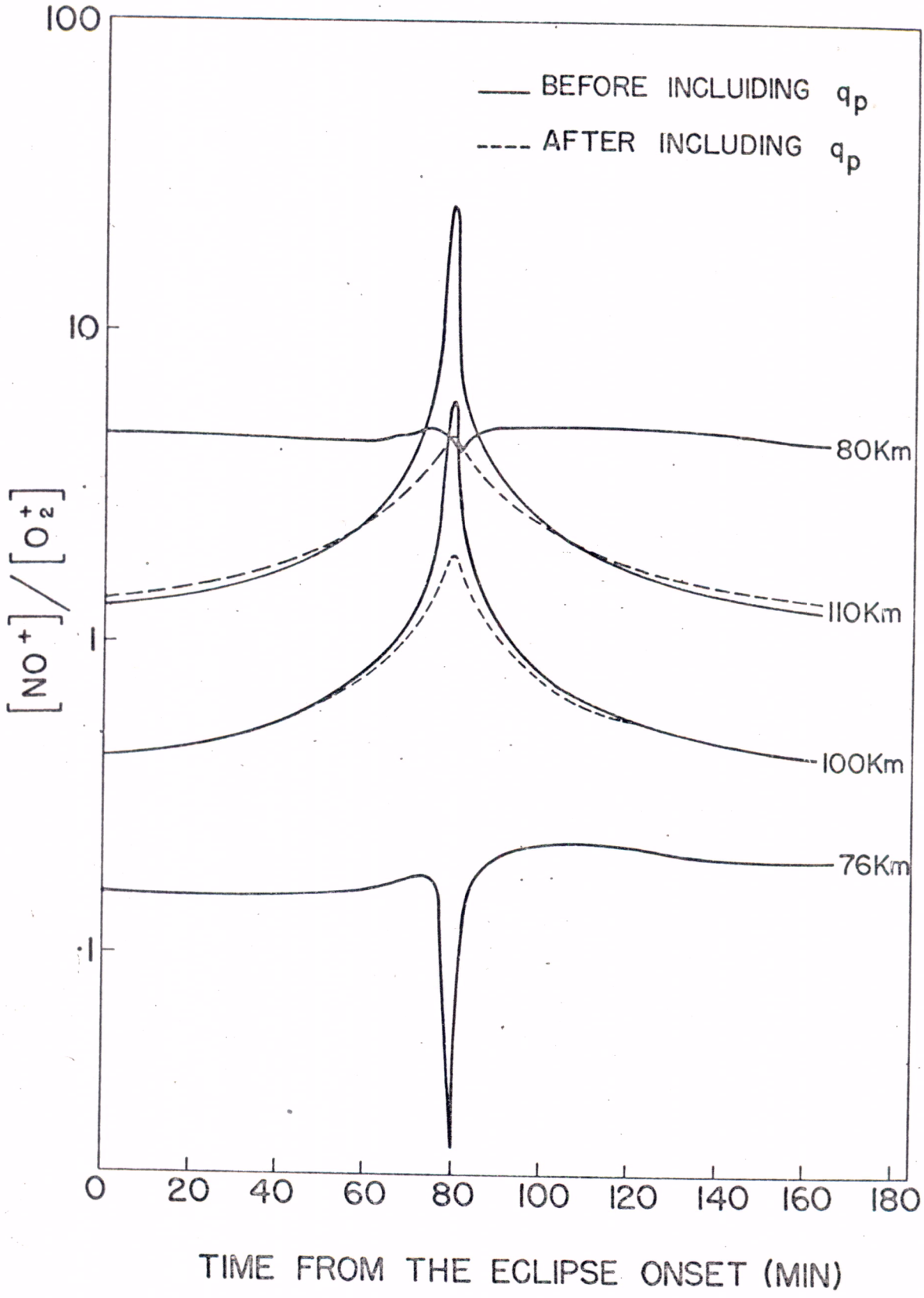

FIG. 6 - Variation of the ratio $[NO^+]/[O_2^+]$ during the eclipse, calculated excluding the q_p (solid line) and including the q_p (broken line).

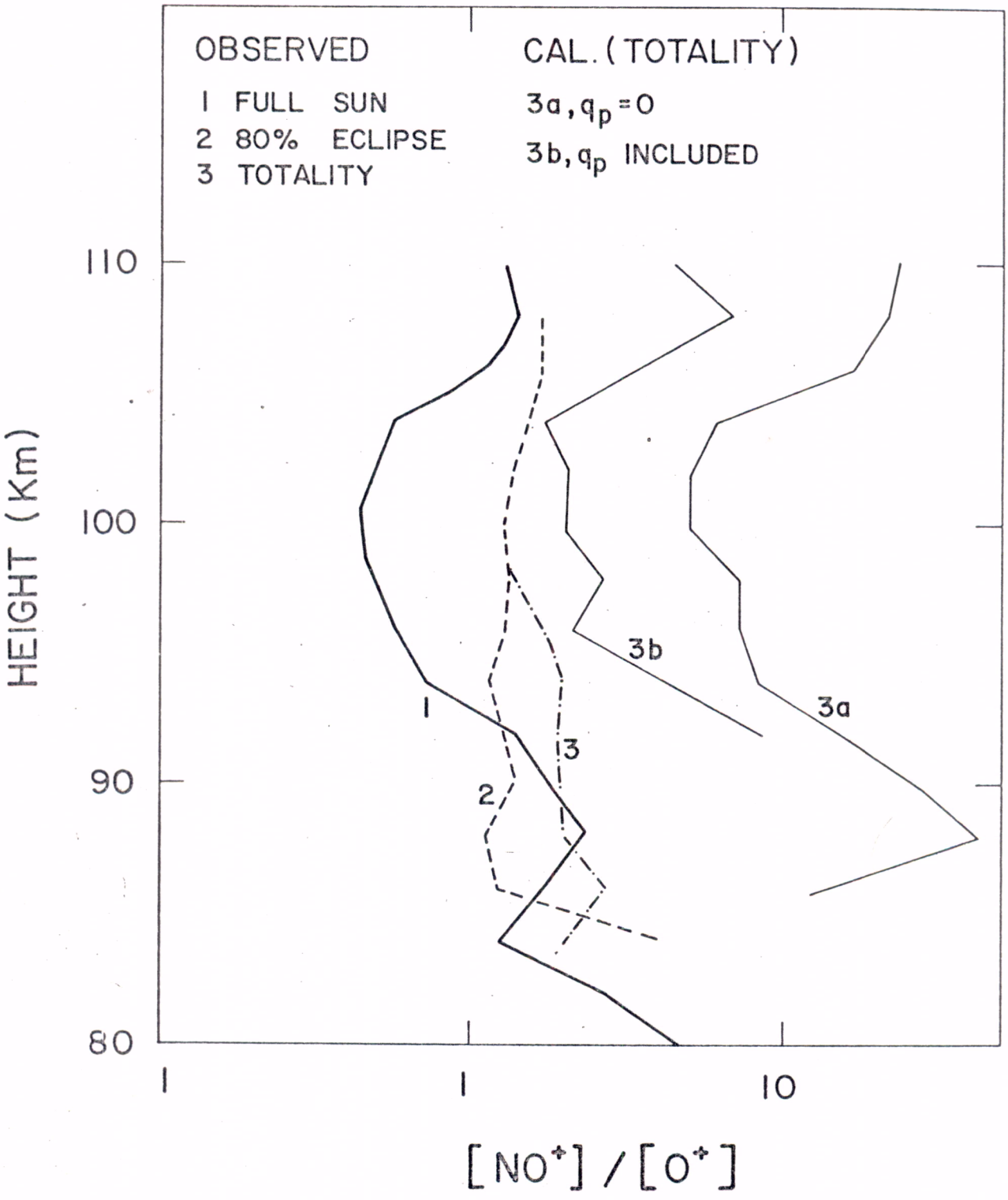

FIG. 7 - Heigth profiles of the ratio $[NO^+]/[O_2^+]$. Curves 1, 2 and 3 represent the measurements by Narcisi et al for the full sun, 80 percent eclipse ant the totality respectively. Curves 3a and 3b represent the calculated results for the totality, excluding the q_p and including the q_p respectively.